



**HAL**  
open science

## A new solvent system: Hydrothermal molten salt

Thomas Voisin, Arnaud Erriguible, Cyril Aymonier

► **To cite this version:**

Thomas Voisin, Arnaud Erriguible, Cyril Aymonier. A new solvent system: Hydrothermal molten salt. *Science Advances*, 2020, 6 (17), pp.eaaz7770. 10.1126/sciadv.aaz7770. hal-02613986

**HAL Id: hal-02613986**

**<https://hal.science/hal-02613986v1>**

Submitted on 2 Jul 2020

**HAL** is a multi-disciplinary open access archive for the deposit and dissemination of scientific research documents, whether they are published or not. The documents may come from teaching and research institutions in France or abroad, or from public or private research centers.

L'archive ouverte pluridisciplinaire **HAL**, est destinée au dépôt et à la diffusion de documents scientifiques de niveau recherche, publiés ou non, émanant des établissements d'enseignement et de recherche français ou étrangers, des laboratoires publics ou privés.

## ENGINEERING

## A new solvent system: Hydrothermal molten salt

T. Voisin<sup>1,2,3</sup>, A. Erriguible<sup>1,2</sup>, C. Aymonier<sup>1\*</sup>

This work proposes a new solvent system composed of a molten salt in pressurized water, so-called hydrothermal molten salt (HyMoS). This system changes the paradigm of the solubility of inorganics in supercritical water. Using as an example NaOH, a low melting temperature salt, we show the possibility to precipitate it at a temperature above its melting one, leading to the instantaneous formation of the HyMoS. The molten salt is then capable of dissolving a large amount of inorganic salt, as exemplified with Na<sub>2</sub>SO<sub>4</sub>. This solvent system opens innovative ways with a potential to impact applications in many fields including materials synthesis, biomass conversion, recycling, green chemistry, catalysis, sustainable manufacturing and others. Beyond the impact on the hydrothermal community, this work also offers previously unexplored opportunities for the molten salt field with access to flow chemistry and insights regarding salt precipitation mechanism.

## INTRODUCTION

On account of the major changes in its thermophysical properties, supercritical water (SCW;  $T > 374^{\circ}\text{C}$ ,  $p > 22.1$  MPa) is sometimes considered as a “magic” solvent (1), as expressed with the example of oil being soluble in SCW. The improvement in terms of kinetics and reactivity, as well as the collapse of polarity, viscosity, and surface tension, widens the potential applications for SCW, such as material synthesis, biomass conversion, or recycling. However, with the polarity breakdown of SCW, the solubility of inorganic compounds drops. Besides the well-known clogging issues due to solid precipitation (2–4), the potential applications with inorganics in hydrothermal environment are also restricted. While organic chemistry in supercritical environment blooms (5), having recourse to inorganic chemicals remains limited because of their very low solubility. One solution could be to identify good cosolvent candidates with great dissolution capacity for inorganic compounds and high thermal stability to overcome SCW limitations.

An attractive possibility would be to have recourse to molten salts, as they usually display high density and important dissolution capacities. When used as reaction medium, molten salts much exhibit high melting temperature, balanced with very low vapor pressure, making their handling quite safe and easy. Molten salt applications are well diversified and have been abundantly used for decades, mainly using nitrate salts (NaNO<sub>3</sub>, KNO<sub>3</sub>...), carbonates (Na<sub>2</sub>CO<sub>3</sub>, K<sub>2</sub>CO<sub>3</sub>...), hydroxides (NaOH, KOH...), or eutectic mixtures for their high capacity to dissolve inorganic material and their thermal stability (6–9). However, molten salts are rarely used in continuous flow systems, as the minimum required working temperature would demand to face strong and costly technical issues. Thus, a chemical process involving injection, pressurization, and mixing of SCW and a molten salt does not seem reasonable.

Still, in the present work, we propose to generate the molten salt within SCW and not only to prove the fact that such a system is processable but also to demonstrate its interest as a serious solution to overcome SCW limitations. This solvent system composed of SCW

and a molten salt, so-called hydrothermal molten salt (HyMoS), is suitable for high-temperature hydrothermal applications and addresses the question of inorganic precipitation in SCW as a fundamental point of view. The HyMoS formation is quite simple: A homogeneous electrolyte water/salt is injected under pressure in the process and heated up. When the temperature reaches the precipitation temperature of the salt, precipitation occurs. As the precipitation temperature is higher than the melting temperature, the precipitation is instantaneously followed by the fusion of the salt, forming the HyMoS (c.f. Fig. 1). In Fig. 1B, the evolution and movement of a molten NaOH droplet can be seen in a sapphire capillary in SCW at 25 MPa and 450°C. After cooling down the system, the initial homogeneous electrolyte water/salt solution is recovered, as the mechanism is completely reversible.

With the aim of demonstrating the interest of the new HyMoS solvent system, the NaOH-Na<sub>2</sub>SO<sub>4</sub> salt system in SCW is considered. The Na<sub>2</sub>SO<sub>4</sub> salt is chosen on account of its well-known behavior and solubility in SCW (10), whereas the NaOH salt is selected for its high thermal stability and low melting temperature (318°C) (11), as well as its high capacity to dissolve inorganic salts. The first section of results dwells on the specific continuous experimental setup that allows the quantification of the solubility of NaOH in SCW and exhibits its molten salt behavior. Subsequently comes the second part, with the NaOH-Na<sub>2</sub>SO<sub>4</sub> system in SCW, where the notable NaOH ability to dissolve solid Na<sub>2</sub>SO<sub>4</sub> particles is highlighted.

## RESULTS

## Molten NaOH solubility in SCW

As previously mentioned, SCW exhibits marked drops in terms of polarity and density leading to the precipitation of inorganic salts due to the decrease in solubility from several orders of magnitude. The idea within this work is to generate the appropriate solvent in situ, illustrated here with molten NaOH, to handle inorganics under SCW conditions. Dissolved inorganics are then carried out with the flow until the low-temperature area where everything redissolves into the water.

With the aim of studying the sodium hydroxide behavior in SCW, we used an experimental setup (c.f. Fig. 2A), which we previously tested on a reference salt and described in details elsewhere (10), to measure solubility values. To be able to measure the solubility of

Copyright © 2020  
The Authors, some  
rights reserved;  
exclusive licensee  
American Association  
for the Advancement  
of Science. No claim to  
original U.S. Government  
Works. Distributed  
under a Creative  
Commons Attribution  
NonCommercial  
License 4.0 (CC BY-NC).

<sup>1</sup>CNRS, Université de Bordeaux, Bordeaux INP, ICMCB, UMR 5026, F-33600 Pessac, France. <sup>2</sup>Bordeaux INP, Université de Bordeaux, CNRS, Arts et Métiers Institute of Technology, INRAE, I2M Bordeaux, F-33600 Talence, France. <sup>3</sup>French Environment and Energy Management Agency, 20 avenue du Grésillé, BP 90406 Angers Cedex 01, France. \*Corresponding author. Email: cyril.aymonier@icmcb.cnrs.fr

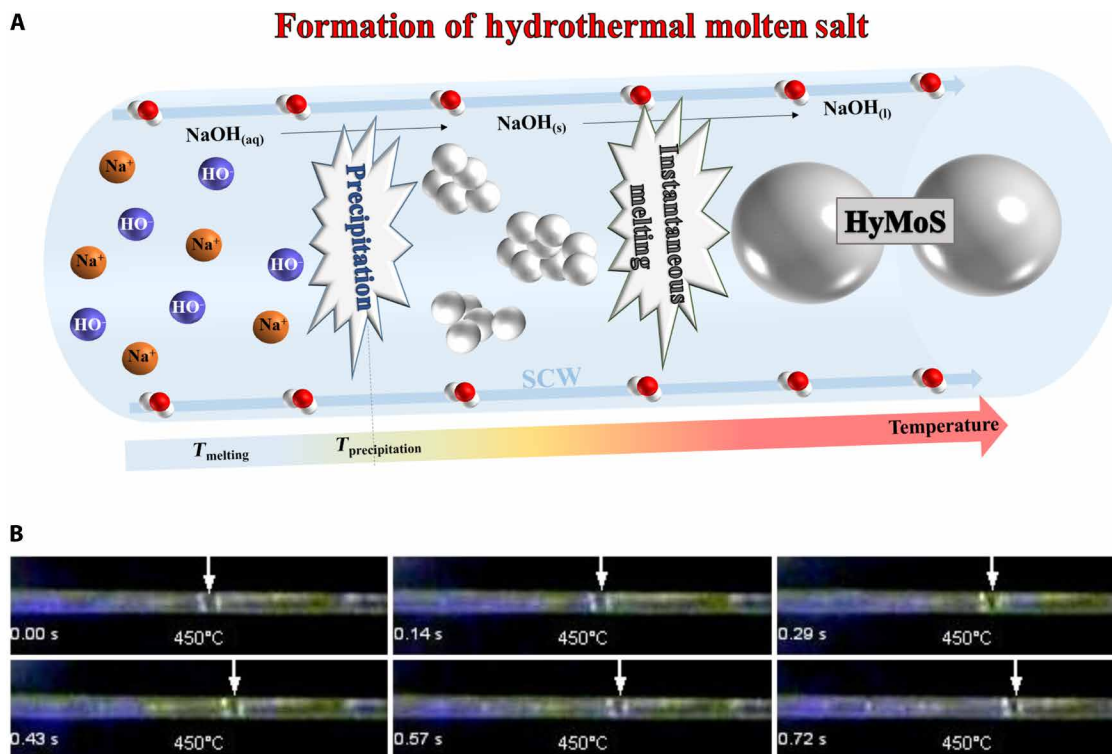


**Fig. 1. Formation of the HyMoS.** (A) Scheme of the formation of the HyMoS in SCW, with the example of NaOH. (B) Montage picture from movie S1 showing the direct observation and movement of a NaOH molten salt droplet in a sapphire capillary at 25 MPa and 450°C. Photo credit: Thomas Voisin, ICMCB.

NaOH under SCW conditions, despite the fact that it is not solid but liquid, the difference in density (12) and viscosity (13) between molten NaOH and SCW was exploited (c.f. Fig. 2, B and C). Because of the use of a large porous media (filter of amorphous carbon particles) and a low flow rate, SCW and molten NaOH do not progress at the same velocity along the filter, ending in a delay between the remaining NaOH concentration in SCW and the initial NaOH concentration (c.f. Fig. 3A). This delay can be detected through the continuous conductivity cell with a decrease in conductivity (c.f. Fig. 3B). Thus, in addition to the conductivity, samples can be taken to perform inductively coupled plasma (ICP) and pH analyses. After a few minutes, the diphasic flow reaches its steady state, and the outlet NaOH concentration comes back to its initial value (c.f. Fig. 3, A and B). Thanks to this dynamic solubility measurement method, we estimated the NaOH solubility curve as a function of temperature at 25 MPa (c.f. Fig. 3C).

It should be noticed that despite the NaOH low melting temperature of 318°C (on which pressure has little influence), the second phase composed of the molten salt does not appear before 380°C to 390°C, corresponding to the precipitation temperature of NaOH. This means that precipitation has to occur before the fusion and the molten NaOH formation. However, it appears that the two-step mechanism of solid precipitation followed by the fusion is sufficiently fast so that no solid particles can be seen in a sapphire capillary equipped with a conventional charge-coupled device camera at 50 fps.

These first results in regard to the molten NaOH demonstrate the feasibility of creating an in situ dense cosolvent, flowing alongside SCW. In addition, we estimated NaOH solubility in SCW through the use of a porous filter, which enables us to tune the molten NaOH fraction in the system as a function of temperature. The next part

brings up the molten NaOH propensity to dissolve other inorganic salts under SCW conditions, a marked change in the paradigm of SCW properties.

#### Na<sub>2</sub>SO<sub>4</sub> solubility in NaOH-based HyMoS

To highlight the NaOH capacity in dissolving solid salt in SCW, we proposed a different experimental protocol. First, we inject an aqueous solution of Na<sub>2</sub>SO<sub>4</sub> in the system at a given temperature, so that solid Na<sub>2</sub>SO<sub>4</sub> salt is deposited on the reactor's wall (c.f. Fig. 4, A and B). As the Na<sub>2</sub>SO<sub>4</sub> solubility is known (10), it can easily be checked whether precipitation occurs in the system due to the continuous conductivity measurements. After 20 to 25 min of Na<sub>2</sub>SO<sub>4</sub> deposition, we switch the feed solution to an aqueous solution of NaOH at a given concentration. Several samples are then taken at the outlet to perform ICP and pH measurements to quantify the NaOH and Na<sub>2</sub>SO<sub>4</sub> concentrations. The point is to evidence a change in the sodium sulfate concentration due to the dissolution of the Na<sub>2</sub>SO<sub>4</sub> solid precipitate in the hydrothermal molten NaOH phase (c.f. Fig. 4C). Samples were taken at different times, different temperatures, and with several NaOH concentrations.

It appears from the first results that, as soon as we inject the NaOH in the system, the first sample exhibits a high concentration of Na<sub>2</sub>SO<sub>4</sub> (c.f. Fig. 4D), which is hundred times the solubility value for this temperature. As time runs, Na<sub>2</sub>SO<sub>4</sub> concentration in the samples decreases, as there is less deposited salt to dissolve inside the reactor. For each sample, NaOH concentration is equal to the feed concentration, following the same behavior as previously exposed (c.f. Fig. 3B).

As the solubility of Na<sub>2</sub>SO<sub>4</sub> and NaOH are known under these conditions, it is possible to calculate the Na<sub>2</sub>SO<sub>4</sub> solubility in the

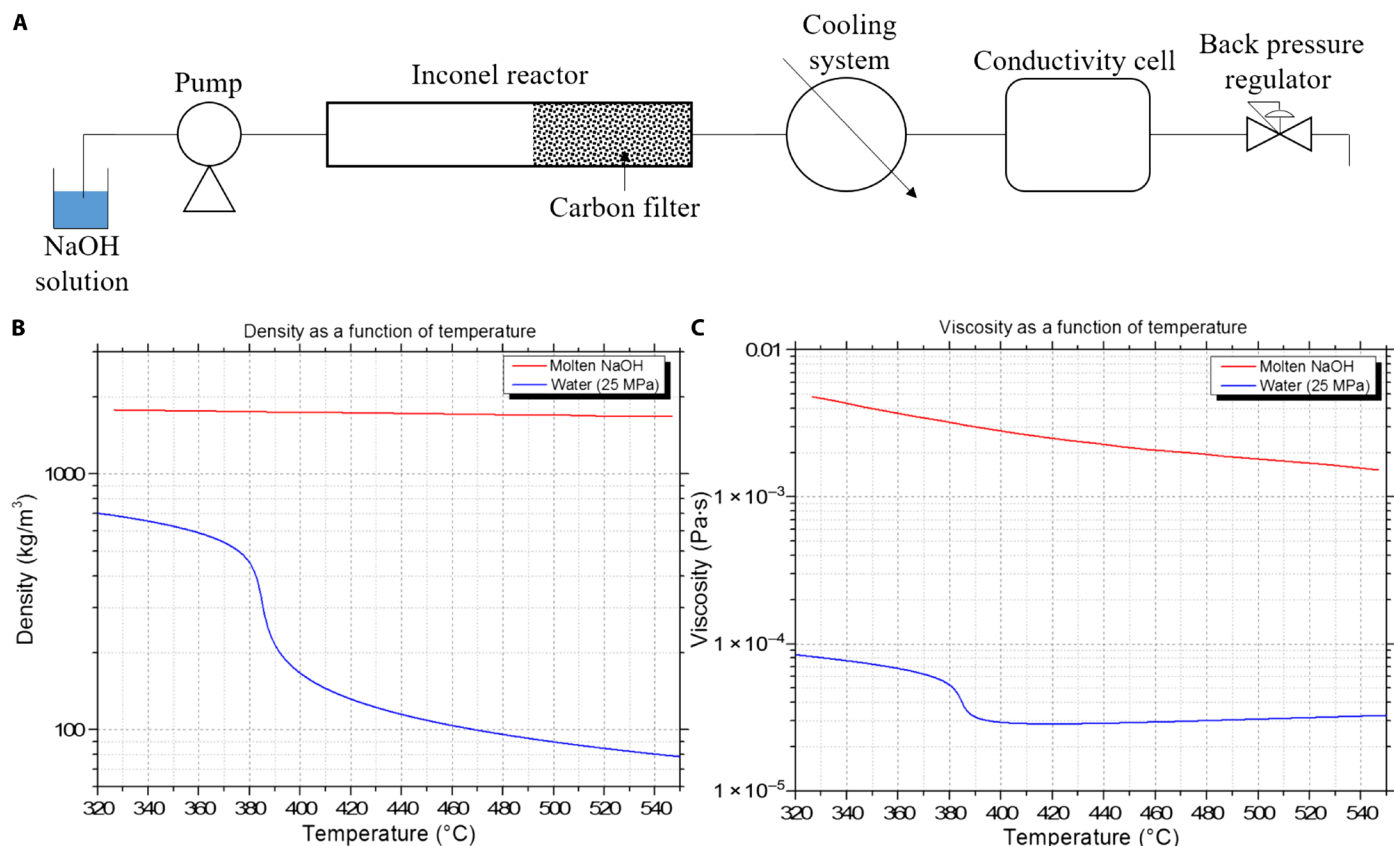


**Fig. 2. Experimental setup used, with comparison between SCW and molten NaOH thermodynamic properties.** (A) Scheme of the experimental setup used for the solubility measurement. (B) Comparison of the density of molten NaOH and water (at 25 MPa), as a function of temperature [reprinted courtesy of the National Institute of Standards and Technology, U.S. Department of Commerce (13). Not copyrightable in the United States. Adapted with permission from (12). Copyright American Chemical Society (1954)]. (C) Comparison of the viscosity of molten NaOH and water (at 25 MPa), as a function of temperature [reprinted courtesy of the National Institute of Standards and Technology, U.S. Department of Commerce. Not copyrightable in the United States (13)].

molten NaOH phase due to the outlet concentration values obtained (c.f. Fig. 4D). Following this, we calculated the  $\text{Na}_2\text{SO}_4$  weight fraction in the NaOH molten phase and plotted it according to the different sampling times, for two different NaOH initial concentrations (c.f. Fig. 4E). Increasing temperature seems to have little influence on the  $\text{Na}_2\text{SO}_4$  concentration in NaOH, whereas the NaOH initial concentration has a major influence on the dissolution rate of the deposited salt. It appears that in the case of an initial concentration of 0.05 M NaOH, a sufficient amount of salt was deposited to saturate the molten NaOH with  $\text{Na}_2\text{SO}_4$ , as the sulfate concentration remains stable at about 40 weight % (wt %) for more than 10 min. When we increased the NaOH feed to 0.1 M, almost all the deposited salt is dissolved in less than 10 min, with a maximum concentration of about 40 wt % in the NaOH molten phase. It is quite logical that as the NaOH feed concentration increases, the NaOH molten phase fraction increases as well, leading to a higher dissolution rate of the deposited salt in the reactor.

According to these results, it seems that the maximum  $\text{Na}_2\text{SO}_4$  solubility in molten NaOH is around 40 wt %, under hydrothermal supercritical conditions at 400° to 420°C and 25 MPa. Regarding the literature of different salt-NaOH binary diagrams, it appears that this saturation limit is in agreement with other order of magnitude for saturation limits [66 wt % for NaCl (14) and 35 wt % for  $\text{Na}_2\text{CO}_3$  (14)] and close to the saturation point of the  $\text{Na}_2\text{SO}_4$ -NaOH diagram

at 410°C at 43 wt % (15). In addition to these results, Ni and Cr quantifications were performed using ICP, to track any corrosion of the reactor due to the high hydroxide concentration. The results showed no signs of corrosion as the amount of Ni and Cr was below the detection limit of the apparatus [ $<1$  parts per million (ppm)].

Direct consequences of these experiments are the potential applications for SCW process, or any hydrothermal process dealing with inorganics, precipitation, and high temperatures. Using a low melting temperature salt, with high thermal stability, enables us to overturn the precipitation issue as an asset. The resulting molten salt acts as a solvent, partially miscible with SCW, and very efficient in dissolving solid inorganics. Instead of being deposited on the reactor's wall, inorganic species are dissolved in the molten salt phase and dragged away with the flow.

## DISCUSSION

These results regarding the behavior of a molten salt in SCW bring and promising opportunities for the molten salts and supercritical fluid-based technologies to address the challenges of our modern society. Using a stable molten hydroxide salt, such as NaOH, enables the generation of an in situ solvent and the dissolution of a large quantity of  $\text{Na}_2\text{SO}_4$  solid salt. This way, we illustrated the first application of HyMoS by the fact that salt deposition and obstruction in

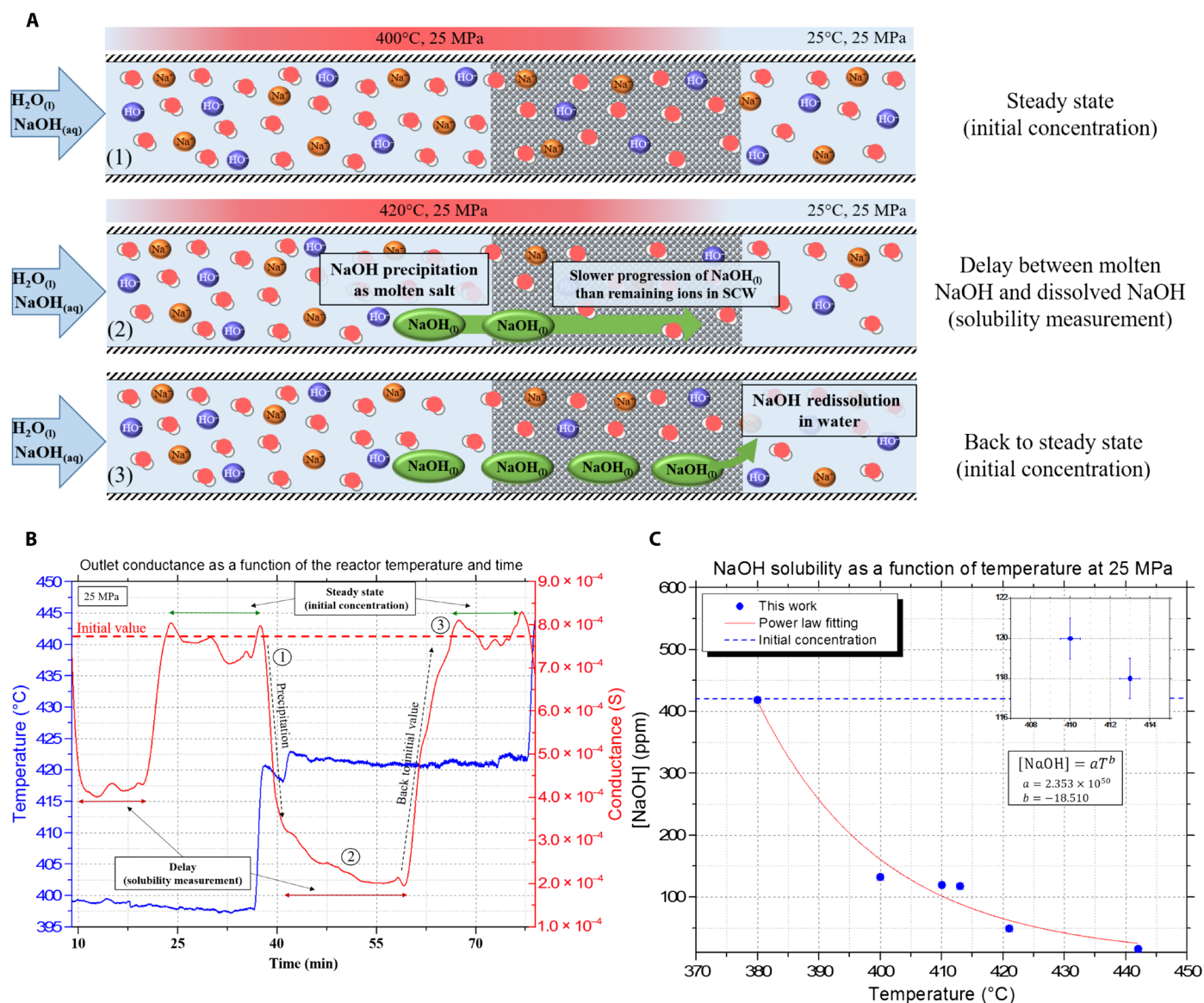


**Fig. 3. Presentation of the continuous conductivity data and the delay, used to measure the NaOH molten salt solubility.** (A) Illustration of the measurement principle using delay analysis due to the viscosity and density differences in the porous media between NaOH and SCW. (B) Example of the continuous measurement obtained with the delay principle, with the blue curve as the temperature inside the reactor and the red line being the conductance measurement at the outlet (corrected from the time delay). (C) Resulting NaOH solubility curve in SCW at 25 MPa.

reactors can be bypassed. Over the past 30 years, great efforts were put into the research and development of specific reactor designs to avoid clogs in SCW processes (16–18). Despite the millions of funding invested (19) and innovative engineering concepts (20–23), one solution could actually be the use of HyMoS to dissolve precipitated inorganics and enables the development of continuous processes. Having recourse to HyMoS would not demand costly investment, as the salt is simply injected in the system in addition to the other products and basic salts such as NaOH are quite cheap materials, compared with complex ionic liquids, for example.

Knowing the solubility of each salt, one can also predict the right amount of NaOH required to dissolve the deposited inorganic salt for an intensive process. Therefore, it is of main interest for SCW processes to take into consideration this new interaction regarding

molten salts and inorganic compounds. The limiting factor of salt precipitation could actually become an asset for the extraction of inorganics using HyMoS and promotes the development of continuous SCW processes.

Beyond the SCW field, the capacity to generate a dense solvent with such a simple and cheap system as H<sub>2</sub>O-NaOH opens a deep reconsideration of the impact and role of high salt content in hydrothermal systems. As expressed previously in this work, application fields for hydrothermal conditions and molten salts are often closely related. However, molten salts can be limited in terms of processability for continuous systems, due to their high viscosity or the high temperatures required, and are often used in batch systems. Having recourse to HyMoS could be an opportunity to develop continuous molten salt-based applications in the fields of material synthesis,

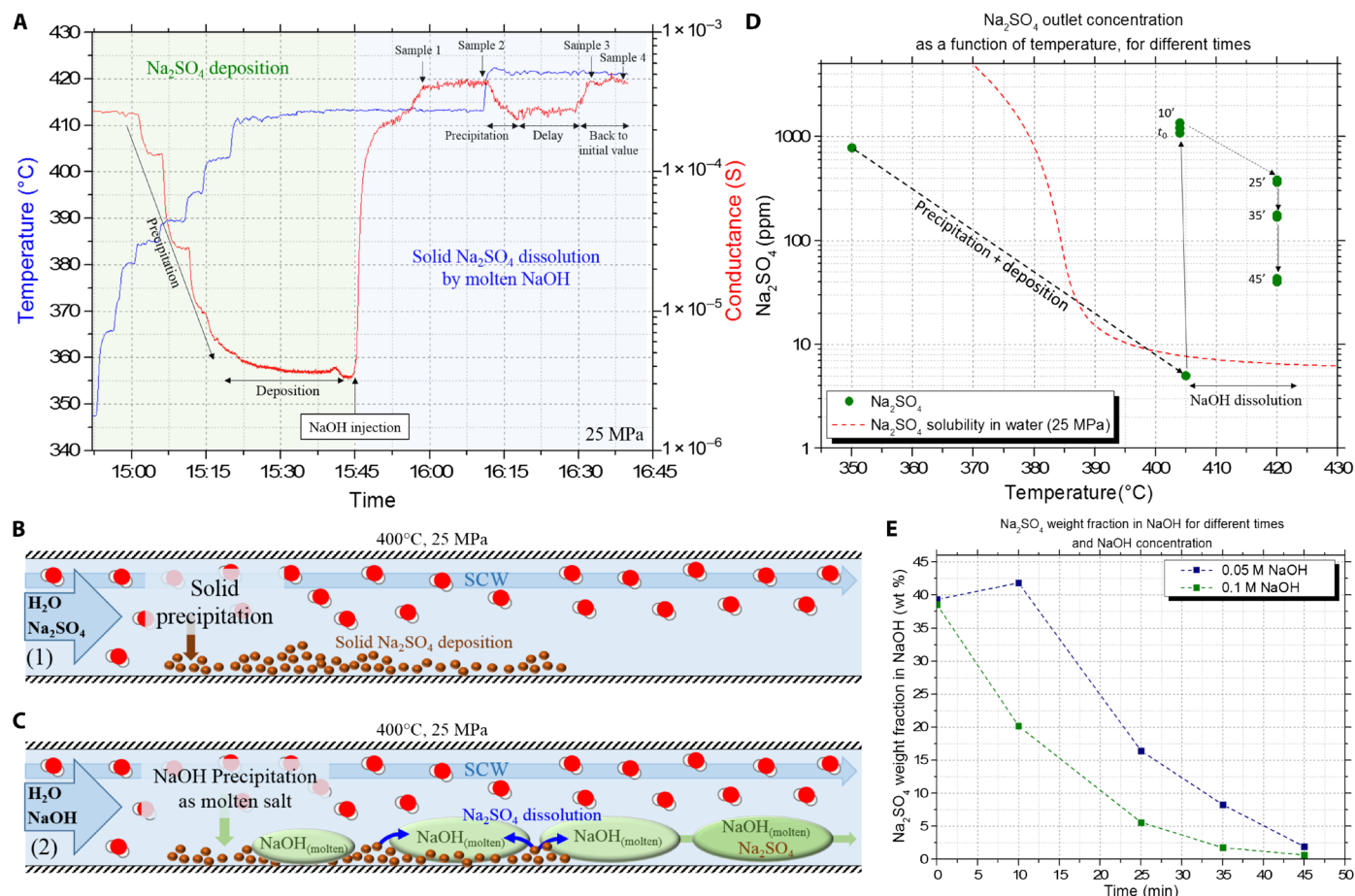


**Fig. 4. Validation of the dissolution of the deposited  $\text{Na}_2\text{SO}_4$  solid salt by the NaOH HyMoS in SCW in continuous flow.** (A) Raw conductance (in red) and temperature (in blue) signals obtained from the experimental setup, showing the different steps of the protocol. Green zone represents the  $\text{Na}_2\text{SO}_4$  precipitation and salt deposition step into the reactor, and blue zone represents the injection of NaOH solution to dissolve the deposited salt. (B) Scheme illustrating the first step of the experiment consisting in salt deposition by precipitation. (C) Scheme illustrating the second step of the experiment, with precipitation/melting of NaOH and the dissolution of the previously deposited  $\text{Na}_2\text{SO}_4$ . (D)  $\text{Na}_2\text{SO}_4$  ICP concentration results according to the temperature, for different times during the dissolution by NaOH. Comparison between the measures and the normal solubility of  $\text{Na}_2\text{SO}_4$  in SCW. (E) Evolution of the  $\text{Na}_2\text{SO}_4$  mass fraction in the NaOH molten phase with time, for two different NaOH feed concentrations.

recycling, or catalysis and to open new routes for inorganic chemistry in supercritical environment. The diphasic system composed of SCW and the molten salt can be used as a new type of hydrothermal water/salt emulsions, of which the droplet structure can be tuned from a segmented flow to an emulsion-like flow, by adjusting the pressure, temperature, and flow velocity (24). This research work was performed regarding NaOH behavior, but several other salts exhibit low melting temperature, below the critical temperature of water (or around 400°C), extending the range of suitable HyMoS systems.

## MATERIALS AND METHODS

### NaOH solubility measurements

For each temperature, we measured NaOH solubility values using an inflow conductivity probe (25–27), confirmed by ICP and pH analyses. We performed ICP on the total sodium content, with an ICP–optical emission spectrometry 720 ES from Varian, whereas for pH measurements, we used a Hanna Instruments probe. We prepared NaOH solutions from solid NaOH pellets, a reagent grade of  $\geq 98\%$ ,

anhydrous, from Sigma-Aldrich with ultrapure water. Our operating conditions and equipment of the continuous conductivity probe are described in details in a previous work (10). Molar conductivity values of sodium hydroxide are taken from literature data (28). We carried out all analyses at an ambient temperature of 20°C.

### $\text{Na}_2\text{SO}_4$ dissolution by NaOH

We prepared sodium sulfate solutions from sodium sulfate powder, ACS grade reagent of  $\geq 99.0\%$ , anhydrous, granular from Sigma-Aldrich, which we dried at 110°C and then dissolved in ultrapure water.  $\text{Na}_2\text{SO}_4$  concentration was 0.005 M for each experiment to ensure a good deposition control in the reactor without massive precipitation, which would clog the system.  $\text{Na}_2\text{SO}_4$  solubility in water at 400°C and 25 MPa is about 3 to 4 ppm (mg/kg).  $\text{Na}_2\text{SO}_4$  deposition is operated for 20 to 25 min with a flow rate of 1 ml/min ( $\pm 0.2$  ml/min). After deposition, we switched the inlet solution from sodium sulfate to sodium hydroxide while keeping the same temperature and pressure conditions in the reactor. We then collected the samples at the outlet during steady states (after NaOH “delays”)

and analyzed them with ICP and pH. We performed ICP measurements on the sulfur and sodium contents to obtain  $\text{Na}_2\text{SO}_4$  and NaOH concentrations. We deduced the sodium sulfate content in the molten NaOH phase from the different concentration values and the known solubility. We assumed that the difference between NaOH initial concentration and its solubility is the quantity of molten NaOH formed. We then supposed that the sodium sulfate dissolved in this NaOH molten phase is the difference between the  $\text{Na}_2\text{SO}_4$  concentration detected and the normal sodium sulfate solubility for the given temperature.

## SUPPLEMENTARY MATERIALS

Supplementary material for this article is available at <http://advances.sciencemag.org/cgi/content/full/6/17/eaaz7770/DC1>

## REFERENCES AND NOTES

1. A. Kruse, N. Dahmen, Water—A magic solvent for biomass conversion. *J. Supercrit. Fluids* **96**, 36–45 (2015).
2. M. Hodes, P. A. Marrone, G. T. Hong, K. A. Smith, J. W. Tester, Salt precipitation and scale control in supercritical water oxidation—Part A: Fundamentals and research. *J. Supercrit. Fluids* **29**, 265–288 (2004).
3. P. A. Marrone, M. Hodes, K. A. Smith, J. W. Tester, Salt precipitation and scale control in supercritical water oxidation—Part B: Commercial/full-scale applications. *J. Supercrit. Fluids* **29**, 289–312 (2004).
4. D. Xu, C. Huang, S. Wang, G. Lin, Y. Guo, Salt deposition problems in supercritical water oxidation. *Chem. Eng. J.* **279**, 1010–1022 (2015).
5. P. E. Savage, Organic chemical reactions in supercritical water. *Chem. Rev.* **99**, 603–622 (1999).
6. G. N. Papatheodorou, Molten salts for two centuries. *Molten Salts Bull.* **83**, 1–6 (2005).
7. D. G. Lovering, *Molten Salt Technology* (Springer, 2014).
8. V. M. B. Nunes, C. S. Queirós, M. J. V. Lourenço, F. J. V. Santos, C. A. Nieto de Castro, Molten salts as engineering fluids—A review: Part I. Molten alkali nitrates. *Appl. Energy* **183**, 603–611 (2016).
9. S. Frangini, A. Masi, Molten carbonates for advanced and sustainable energy applications: Part II. Review of recent literature. *Int. J. Hydrogen Energy* **41**, 18971–18994 (2016).
10. T. Voisin, A. Erriguible, G. Philippot, D. Ballenghien, D. Mateos, F. Cansell, B. B. Iversen, C. Aymonier, Investigation of the precipitation of  $\text{Na}_2\text{SO}_4$  in supercritical water. *Chem. Eng. Sci.* **174**, 268–276 (2017).
11. CDC - SODIUM HYDROXIDE - International Chemical Safety Cards - NIOSH; [www.cdc.gov/niosh/topics/sodium-hydroxide/](http://www.cdc.gov/niosh/topics/sodium-hydroxide/).
12. D. Bogart, Densities of molten sodium and rubidium hydroxides. *J. Phys. Chem.* **58**, 1168–1169 (1954).
13. G. J. Janz, F. W. Dampier, G. R. Lakshminarayanan, P. K. Lorenz, R. P. T. Tomkins, *Molten Salts: Volume 1, Electrical Conductance, Density, and Viscosity Data* (U.S. Government Printing Office, 1968).
14. G. J. Janz, R. P. T. Tomkins, Molten salts: Volume 5, part 2. Additional single and multi-component salt systems. Electrical conductance, density, viscosity and surface tension data. *J. Phys. Chem. Ref. Data.* **12**, 591 (1983).
15.  $\text{Na}_2\text{SO}_4$ -NaOH binary diagram. FactsSage database; [factsage.com](http://factsage.com).
16. M. D. Bermejo, M. J. Cocero, Supercritical water oxidation: A technical review. *AIChE J.* **52**, 3933–3951 (2006).
17. G. Brunner, Near critical and supercritical water. Part I. Hydrolytic and hydrothermal processes. *J. Supercrit. Fluids* **47**, 373–381 (2009).
18. C. Aymonier, M. Bottreau, B. Berdeu, F. Cansell, Ultrasound for hydrothermal treatments of aqueous wastes: Solution for overcoming salt precipitation and corrosion. *Ind. Eng. Chem. Res.* **39**, 4734–4740 (2000).
19. V. Vadillo, J. Sánchez-Oneto, J. R. Portela, E. J. Martínez de la Ossa, Problems in supercritical water oxidation process and proposed solutions. *Ind. Eng. Chem. Res.* **52**, 7617–7629 (2013).
20. H. Roche, M. Weber, C. Trepp, Design rules for the wallcooled hydrothermal burner (WHB). *Chem. Eng. Technol.* **20**, 208–211 (1997).
21. B. Wellig, K. Lieball, R. von Rohr, Operating characteristics of a transpiring-wall SCWO reactor with a hydrothermal flame as internal heat source. *J. Supercrit. Fluids* **34**, 35–50 (2005).
22. M. J. Cocero, J. L. Martínez, Cool wall reactor for supercritical water oxidation: Modelling and operation results. *J. Supercrit. Fluids* **31**, 41–55 (2004).
23. D. H. Xu, S. Z. Wang, Y. M. Gong, Y. Guo, X. Y. Tang, H. H. Ma, A novel concept reactor design for preventing salt deposition in supercritical water. *Chem. Eng. Res. Des.* **88**, 1515–1522 (2010).
24. F. Zhang, A. Erriguible, T. Gavoille, M. T. Timko, S. Marre, Inertia-driven jetting regimes in microfluidic coflows. *Phys. Rev. Fluids* **3**, 092201 (2018).
25. M. S. Gruszkiewicz, R. H. Wood, Conductance of dilute LiCl, NaCl, NaBr, and CsBr solutions in supercritical water using a flow conductance cell. *J. Phys. Chem. B* **101**, 6549–6559 (1997).
26. P. C. Ho, H. Bianchi, D. A. Palmer, R. H. Wood, Conductivity of dilute aqueous electrolyte solutions at high temperatures and pressures using a flow cell. *J. Solution Chem.* **29**, 217–235 (2000).
27. G. H. Zimmerman, P. W. Scott, W. Greynolds, A new flow instrument for conductance measurements at elevated temperatures and pressures: Measurements on NaCl(aq) to 458 K and 1.4 MPa. *J. Solution Chem.* **36**, 767–786 (2007).
28. K. N. Marsh, R. H. Stokes, The conductance of dilute aqueous sodium hydroxide solutions from 15° to 75°. *Australian J. Chem.* **17**, 740–749 (1964).

### Acknowledgments

**Funding:** We acknowledge financial support from the INNOVOX Company and the French Environment and Energy Management Agency (ADEME). **Author contributions:** T.V., A.E., and C.A. contributed equally to this work. **Competing interests:** C.A., T.V., and A.E. have a priority patent no. FR 1760895 filed on 17 November 2017, published on 24 May 2019 (number 307354) and extended by PCT, application no. EP2018081652 on 16 November 2018. Ecole Nationale Supérieure des Arts et Métiers, Université de Bordeaux, Institut Polytechnique de Bordeaux. The authors declare that they have no other competing interests. **Data and materials availability:** All data needed to evaluate the conclusions in the paper are present in the paper and/or the Supplementary Materials. Additional data related to this paper may be requested from the corresponding author.

Submitted 8 October 2019

Accepted 3 February 2020

Published 24 April 2020

10.1126/sciadv.aaz7770

**Citation:** T. Voisin, A. Erriguible, C. Aymonier, A new solvent system: Hydrothermal molten salt. *Sci. Adv.* **6**, eaaz7770 (2020).

## A new solvent system: Hydrothermal molten salt

T. Voisin, A. Erriguible and C. Aymonier

*Sci Adv* **6** (17), eaaz7770.  
DOI: 10.1126/sciadv.aaz7770

### ARTICLE TOOLS

<http://advances.sciencemag.org/content/6/17/eaaz7770>

### SUPPLEMENTARY MATERIALS

<http://advances.sciencemag.org/content/suppl/2020/04/20/6.17.eaaz7770.DC1>

### REFERENCES

This article cites 24 articles, 0 of which you can access for free  
<http://advances.sciencemag.org/content/6/17/eaaz7770#BIBL>

### PERMISSIONS

<http://www.sciencemag.org/help/reprints-and-permissions>

Use of this article is subject to the [Terms of Service](#)

---

*Science Advances* (ISSN 2375-2548) is published by the American Association for the Advancement of Science, 1200 New York Avenue NW, Washington, DC 20005. The title *Science Advances* is a registered trademark of AAAS.

Copyright © 2020 The Authors, some rights reserved; exclusive licensee American Association for the Advancement of Science. No claim to original U.S. Government Works. Distributed under a Creative Commons Attribution NonCommercial License 4.0 (CC BY-NC).